Results in Engineering 23 (2024) 102844

Contents lists available at ScienceDirect

Results in Engineering

journal homepage: www.sciencedirect.com/journal/results-in-engineering

Experimental analysis of low-duty cycle campus deployed IoT network using LoRa technology

Gagandeep Kaur [a], Vipin Balyan [b], Sindhu Hak Gupta [a,*]

[a] Department of Electronics and Communication Engineering, Amity University, Sector-125, Noida, India
[b] Department of Electrical, Electronics and Computer Engineering, Cape Peninsula University of Technology, Cape Town, South Africa

ARTICLE INFO

Keywords:
IoT
LPWAN
LoRa
Link quality
Reliability

ABSTRACT

This study emphases on the implementation and evaluation of a LoRa network in indoor environments through an experimental setup at Amity University, Greater Noida (AUGN) campus. Aimed at scrutinizing the link-level performance and reliability of LoRa technology, extensive measurements have been conducted with prototype device integrating the SX1278 LoRa radio module at 433 MHz. The performance has been analysed in terms of Signal-to-Noise Ratio (SNR), Received Signal Strength Indicator (RSSI), and Packet Reception Rate (PRR) across various line-of-sight (LoS) and non-line-of-sight (NLoS) scenarios. The results reveal that network performance is highly sensitive to parameter configurations, such as spreading factor (SF) and coding rate (CR). In LoS environments, SF = 9 and CR = 4/5 provided an RSSI of −89.12 dBm and an SNR of 9.91 dB, while highly obstructive areas saw optimal performance with SF = 7 and CR = 4/7. The study also identified configurations ensuring 100 % packet delivery accuracy and maximum throughput. This work stands out due to its thorough examination of LoRa for indoor IoT applications, notably addressing duty cycle restrictions, a topic often overlooked in existing literature. The valuable insights presented are crucial for maximizing the potential of LoRa in indoor environments with high population density. The findings strongly advocate for the use of LoRa for real-time environmental monitoring and innovative IoT applications within university campuses.

1. Introduction

Advancements in wireless technologies are driven to enhance spectrum utilization, data rate, communication range, and battery lifetime. Innovations in technology and pervasive connectivity have piloted the emergence of the Internet of Things (IoT) concept. The IoT market is anticipated to escalate to over $1.8 trillion by 2028 [1]. IoT-based systems typically involve physical devices embedded with sensors and processors broadcasting data over the network assisting in management/monitoring applications in various domains [2]. The quintessential requirement is that the deployed devices should consume less power and linger over the same battery for more than 10 years covering a large geographical area [3].

For indoor IoT applications, several wireless technologies are commonly considered. The reigning short-range wireless standards represented by IEEE 802.11 (WiFi), IEEE 802.15.1 (Bluetooth), IEEE 802.15.4 (ZigBee) and such, operating over 2.4 GHz Industrial, Scientific and Medical (ISM) bands provide high data rates but are limited in use for many IoT applications due to shorter geographical coverage and high-power consumption.

Specifically designed for IoT applications, Wi-Fi HaLow and Bluetooth Low Energy (BLE) offer lower power consumption and extended range compared to their traditional counterparts, making them suitable for indoor environments. Wi-Fi HaLow, operating in the sub-1 GHz band, provides extended range and improved penetration through obstacles, while BLE focuses on short-range communication with minimal power use [4].

On the counterpart, cellular technologies represented by 3G, 4G and imminent 5G provide larger geographical coverage and high data rate and cater to IoT applications at a fairly high cost due to their operation in a licensed band and high-power consumption [5]. Most IoT applications do not require a high data rate as they transmit occasionally but necessitate lower latency and low operational costs. This persuaded the existence of Low Power Wide Area Network (LPWAN) technologies [6].

LPWAN technologies channel the breach between short-range and cellular technologies, offering a large communication range at low power expenditure and cost [7]. Long Term Evolution for Machines (LTE-M), NB-IoT, EC-GSM and LTE-M take the advantage of already

* Corresponding author.
E-mail addresses: gaganksodhi@gmail.com (G. Kaur), vipin.balyan@rediffmail.com (V. Balyan), shak@amity.edu (S.H. Gupta).

https://doi.org/10.1016/j.rineng.2024.102844
Received 14 March 2024; Received in revised form 11 August 2024; Accepted 2 September 2024
Available online 4 September 2024

existing installed infrastructure of traditional cellular networks expanding the coverage but having the drawback of high operational costs working in the licensed band. The advantages of Sigfox and LoRa operating in the unlicensed band are low deployment cost and low power consumption. Coverage and capacity comparison made in Ref. [8] between LoRa and Sigfox and the absence of uplink acknowledgement signals in Sigfox [9] presents LoRa as a more suitable LPWAN candidate.

With this aspect, the current work intends to utilize the LoRa technology to deploy a real-time monitoring system in large and crowded indoor areas for smart IoT applications. Although LoRa is primarily designed for long-range communication, its benefits in indoor environments include robust penetration through obstacles and low power consumption, making it a superior choice over other IoT technologies like Wi-Fi HaLow and BLE for certain applications. To enable LoRa technology in an indoor area for gathering real-time environmental monitoring data for pioneering IoT applications, the network has been set up on a university campus. The deployed network comprises the sensors to monitor the environmental vitals such as temperature and humidity. The deployed network serves as a platform to facilitate the development of diverse IoT applications which could include mobile IoT applications to monitor real-time information for maintenance plans, and assist in engaging campus premises for teaching accomplishments or self-study.

Thus, the current work emphasizes on studying the link level performance and evaluating the reliability of this technology aiming to scrutinize the effect of various transmission parameters on the network performance for the same coverage area considering various environmental scenarios. The link-level performance of the IoT network based on LoRa technology deployed on a university campus is explored in terms of Received Signal Strength Indicator (RSSI), Signal-to-Noise Ratio (SNR) and Packet Reception Rate (PRR). This has been achieved through rigorous experiments done indoors covering different environments such as line-of-sight, obstructive and highly obstructive.

The significant offerings of the current work are.

1. Experimentally studying the link-level performance of LoRaWAN-based low-duty cycle IoT network in terms of RSSI and SNR covering different environmental scenarios.
2. Analyzing the reliability of the setup network by evaluating PRR and throughput utilizing the recorded measurements.

The remaining paper is recapitulated as: In section 2, some related deployments of the LoRa network for various IoT applications have been discussed followed by a brief about LoRa technology in section 3. The experimental setup used for the study is described in section 4 with its measurement methodology in section 5. The measurement outcomes are discussed in section 6 and section 7 concludes the current study.

2. Related work

Currently, numerous studies have employed wireless communication networks for IoT-based indoor environmental monitoring of large area smart buildings. Wireless communication technologies, ranging from Bluetooth and radio frequency for short distances to 3G, ZigBee, and LoRa for medium and long distances, have shown progressively encouraging impressions on indoor environment monitoring systems.

Cho et al. [10] and Smith et al. [11] utilized Bluetooth for indoor environment monitoring but necessitated close proximity to sensing nodes and thus can be a limitation for large spaces. Addressing this, Tran et al. established an RFID tag device for data collection within 250 cm of the reader [12]. WiFi-enabled sensing nodes have also been deployed for indoor monitoring, as seen in studies by Martín-Garín et al. [13] and Moreno-Range et al. [14] that deployed a WiFi-enabled sensing node in a room where as Yang et al. [15] carried out office experiments for monitoring purposes. Carre et al. took a different approach and utilized a 3G-enabled device with a SIM card for internet connectivity and deployed in a lounge for monitoring experiments [16].

The preference for wireless communication networks in IoT-based monitoring is driven by their capability to condense wiring complexity. While Bluetooth and RF are restricted by their short range, WiFi and 3G networks provide greater flexibility. However, considerations for building support and access traffic are crucial for successful deployment.

ZigBee technology then emerged as a promising solution for medium-range indoor monitoring. Karami et al. [17] conducted a successful deployment of two ZigBee module nodes and a coordinator in a laboratory setting to continuously collect indoor environmental data over a period of 10 days, with no missing data recorded. Additionally, Yang et al. [18] utilized a network of ten transmitting nodes within a university environment to assess data across multiple buildings, effectively utilizing ZigBee technology for data transmission. An extensive amount of research has been done on LoRa technology catering to IoT applications. Zhibin Liu. et al. in Ref. [19] provides a comprehensive performance analysis of ZigBee and LoRa technologies in entire structure under identical conditions. The conclusions demonstrate that LoRa networks consistently outdo ZigBee networks, making them the superior choice for establishing communication networks.

The contemporary IEEE 802.11ah standard, known as Wi-Fi HaLow [20], is designed to provide long-range data links and reduced power consumption in the sub-GHz bands. The performance of Wi-Fi HaLow has been subject to several theoretical studies, as there are presently not much existing devices for practical evaluation. The study in Ref. [20] presents testbed performance analysis that assess the network performance of Wi-Fi HaLow focusing on throughput, latency, and reliability, comparing it with IEEE 802.11n (Wi-Fi n) and the IoT technology LoRa. For distances exceeding 1 km with no LoS, Wi-Fi HaLow has limitations, while LoRa performs better and is more reliable.

Another powerful technology is BLE technology that utilizes the RSSI value to enable real-time localization and has many advantages such as low energy usage and cost-effectiveness [21]. However, it is highly susceptible to fast fading and has a higher packet drop rate in close proximity and when blocked by building elements. LoRa signals have better penetration and stability compared to WiFi and BLE, making it a promising alternative for indoor localization.

LoRa technology is majorly focused due to its openness and readily available hardware that can be customized for experimental study and hasty prototyping. M.O. Ojo et al. in Ref. [22] focused on the employment of LoRa LoRa-based IoT network and evaluated the performance of the LoRaWAN network operating at 433 MHz and 868 MHz ISM band. O. Elijah et al. in Ref. [23], experimentally studied the impact of weather conditions on the LoRaWAN communication. The research in Ref. [24] provided a comprehensive performance evaluation of LoRaWAN communication concerning the Doppler effect between vehicle-to-infrastructure (V2I), vehicle-to-vehicle (V2V) and stationary vehicles through simulations and field measurements. K. Lin et al. in Ref. [25] investigated the link quality of the LoRaWAN communication in a wireless underground sensor network (WUSN).

S. Mehdi et al. in Ref. [26] performed the link analysis of LoRaWAN for the reception of data packets at an altitude with an elevation angle of maximum 0°. Q. Guo et al. in Ref. [27], the authors provide the impact of different LoRa transmission parameters settings and packet length on the performance of the LoRa network through trial measurements. P. Kulkarni et al. in Ref. [28], studied the link level performance and coverage of the LoRa technology deployed on university campus focusing on different indoor and outdoor locations. M. J. Faber et al. in Ref. [29] evaluated the performance of outdoor obstructive environments in terms of link quality. R. Liang et al. in Ref. [30], the authors explored the LoRaWAN performance in a multistorey building. Focusing on evaluating the coverage and time measurement capabilities of the LoRa device, A. Vazquez-Rodas et al. in Ref. [31] analysed the LoRaWAN performance through field measurements.

Boubaker Abdallah et al. in Ref. [32], investigated the reliability of the LoRa network under NLoS and noisy and mobile indoor industrial environment. The reliability of the network has been estimated to be 90.23 % emphasizing on specific LoRa configurations. Nelson Carvalhal Lopes et al. in Ref. [33], developed an indoor monitoring system based on LoRa network. In depth study of the system has been carried out using test-bed analysis to assess the performance in terms of RSSI. L. Aarif et al. in Ref. [34]evaluated the LoRa network performance by eliminating the forward error correction in harsh industrial environment. The SNR performance has been boosted using FIR filters depending upon the simulation parameters.

Ricardo Robles-Enciso et al. in Ref. [35], presented the power and link quality measurements of LoRa, Zigbee and 5G network. Their performance has been evaluated focusing on RSSI and BER. It has been established that LoRa and Zigbee yields BER than 5 %. RSSI values indicated the better performance of LoRa than other technologies in indoor corridor environments. The study in Ref. [36], demonstrates the potential of using LoRa technology for smart home applications. It includes an LoRa home area network, a cloud-based server, and a mobile application. The methodology analyzes the LoRa transmission delay, communication distance, and link quality, considering various barriers. Additionally, the study explores indoor signal propagation modeling, accounting for multipath signals through the Rayleigh and Rician distributions.

The motivation for this work comes from the discussions mentioned above and the authors' aim to comprehensively investigate LoRa network performance under varying simulation parameters in the same coverage area and across different environmental scenarios. The current work focuses on evaluating the link quality and reliability of the network for the same coverage area under different configurations and environmental scenarios.

This work introduces duty cycle restrictions, an overlooked aspect in similar studies, adding to its novelty. Therefore, to adhere to the maximum duty cycle constraints directed by regional regulations for LoRa devices, the maximum number of messages sent per hour has been decreased. Furthermore, while LoRa's capabilities of large coverage has been well-documented, our study aims to investigate its performance in an indoor environment for distance not exceeding 100 m. By examining these variables, we target to gain a clearer understanding of how different configurations, environmental conditions, and duty cycle constraints influence the network's performance.

A summarized related deployment of the LoRaWAN network for various IoT applications in different environmental scenarios has been stated in Table 1. In the present work, link-level performance, and reliability of the LoRa-based IoT network deployed in a university campus have been explored. This has been accomplished through extensive experiments in an indoor campus environment covering line-of-sight (LoS) and non-line-of-sight (NLoS) environments.

Table 1
Comparison of related work.

Reference	LoRa Module	Frequency band	Environmental Scenarios	Performance Metrics
[22]	LoRa RN2483 embedded with Semtech SX1276	433 MHz, 868 MHZ	Outdoor-obstructive	RSSI, SNR, PDR
[23]	Semtech SX1272	923 MHz	Outdoor-less obstructive	RSSI
[24]	Semtech SX1276	915 MHz	Outdoor-LoS, obstructive	RSSI, SNR, PDR
[25]	Semtech SX1278, SX1301	433 MHz	Outdoor-obstructive	RSSI, SNR, PDR
[26]	Semtech SX1278	433 MHz	Outdoor-obstructive	RSSI, SNR
[27]	LoRa RN2483 embedded with Semtech SX1276	433 MHz, 868 MHz	Indoor-LoS	PRR
[29]	Semtech SX1301	902–903 MHz	Outdoor- LoS, obstructive	RSSI, SNR
[30]	Semtech SX1278	433 MHZ	Indoor- LoS and obstructive	RSSI, SNR, PDR
[31]	Semtech SX1272	868 MHz	Outdoor-obstructive	RSSI
[32]	USRP N321	169.7 MHz.	Indoor -NLoS	BLER, SINR, data rate
[33]	Semtech SX1276	868 MHz	Indoor- LoS and obstructive	RSSI
[34]	LoRa PyCom	868 MHz	Indoor- LoS and obstructive	RSSI, BER
[35]	Semtech SX1278	433 MHz	Indoor- LoS and obstructive	RSSI, PRR
[36]	Waspmote LoRa board	868 MHz	Indoor; Outdoor-LoS, obstructive	RSSI, PDR
Current work	Semtech SX1278	433 MHz	Indoor- LoS, obstructive, highly obstructive	RSSI, SNR, PRR, Throughput

3. LoRa technology

LoRa technology is based on open standards supported by open-source implementation facilitating rapid acceptance across the globe. LoRa technology was developed by Semtech for low-power, extended-coverage IoT applications [37]. LoRa operates on 433 MHz, 868 MHz and 915 MHz bands utilizing the unlicensed ISM bands. LoRa has acquired major consideration from academics and researchers due to its readily available hardware in the market that can be customized to improve energy consumption and link-level performance. It has a striking attribute of adjusting its transmission parameters at the device level: Spreading Factor (SF), Coding Rate (CR), bandwidth, carrier frequency and transmitted power [38]. This eases experimental research and hasty modelling.

Above the physical layer lies the LoRaWAN link layer standardized by LoRa Alliance. LoRaWAN utilizes the ALOHA medium access control (MAC) scheme to access the unlicensed channel. LoRaWAN deployments are exposed to rigorous limitations to the utilization of the ISM band in many regions of the world. The maximum extent of time the LoRa devices are permitted to occupy the ISM band is stated in terms of the duty cycle (DC). The duty cycle ranges from 0.1 % to 10 %. The maximum allowable duty cycle for the LoRa device on the 433 MHz ISM band is 10 %. This means that not more than 8640 s can be given to the LoRa device to occupy the radio channel per day. Due to duty cycle restrictions, the device goes into a sleep period after transmitting a frame. This renders a delay between two consecutive LoRa frames. When a device transmits a packet, the system goes to sleep period (T_s) and wait for $T_s = T_a\left(\frac{1}{DC} - 1\right)$ secs before transmitting the next packet on the same channel. The duty cycle restrictions result in a restrained number of transmissions allowed per day by a LoRa device [39]. For DC = 10 %, the maximum permitted time is 360 s/h. Thus, the maximum permitted transmissions per hour can be calculated as $n = {}^{360}/_{T_a}$. Time on air (T_a) is the packet transmission duration and is determined by adding the preamble duration and the payload duration as expressed by equation (1) [40].

$$T_a = T_{preamble} + T_{payload} \tag{1}$$

The LoRa frame begins with a preamble of default size 8 bytes ($n_{preamble}$) exercised for synchronizing the transmitter and receiver. Preamble duration is expressed as

$$T_{preamble} = \left(n_{preamble} + 4.25\right) \times \frac{2^{SF}}{BW} \tag{2}$$

The payload duration relates to the duration of number of symbols

($N_{payload}$) used to transmit a given payload (PL) in bytes. These number of transmitted symbols are calculated as

$$N_{payload} = 8 + \left(ceil\left(\frac{8PL - 4SF + 28 + 16CRC - 20H}{4(SF - 2DE)} \right)(CR + 4), 0 \right) \tag{3}$$

where, H = 0 when header enabled otherwise 1; DE = 1 for enabled low data rate optimization otherwise 0; CRC = 1 when enabled otherwise 0 [41]. Thus, the payload duration can be given as

$$T_{payload} = N_{payload} \times \frac{2^{SF}}{BW} \tag{4}$$

Fig. 1 illustrates the influence of SF and CR on the permissible number of transmissions per day for a payload size of 44 bytes and BW = 125 kHz. The figure illustrates that the maximum number of transmissions per day is 166670 packets for SF = 7 and CR = 4/8. However, the minimum is for SF = 12 & CR = 4/5 with the number of transmissions to be not more than 8310 packets per day. Fig. 2 shows the impact of CR and SF on time on air for a payload size of 44 bytes and BW = 125 kHz. In our LoRa setup, to prevent surpassing the LoRaWAN duty cycle restrictions and provide efficient performance, the experiment has been conducted with the system measuring and sending LoRa packet after every 10 min.

4. Experimental setup

To study the link quality and reliability of the LoRaWAN communication as a function of LoRa transmission configuration for collecting real-time monitoring data, a series of indoor tests are conducted. All the experiments are conducted at Amity University, Greater Noida (AUGN) campus, India (28.4651° N, 77.4845° E). An indoor gateway has been set up in a laboratory of the engineering block of the AUGN campus while the prototype LoRa end device is deployed at different locations in the campus to cover various propagation environments.

4.1. Hardware setup

The measurement set-up consists of a prototype LoRa device sensing the monitoring data i.e. temperature and humidity and a LoRa gateway connected to a laptop as an interface to control the received messages. The prototype device integrates the LoRa SX1278 radio module manufactured by Semtech operating in the 433 MHz ISM band. Fig. 3 shows the LoRa end device equipped with a DHT11 sensor for measuring temperature and humidity, a LoRa radio module for communication and

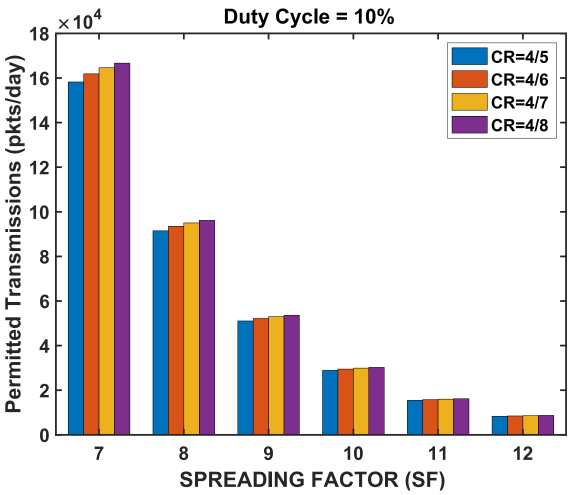

Fig. 1. Permitted transmissions for various values of SF.

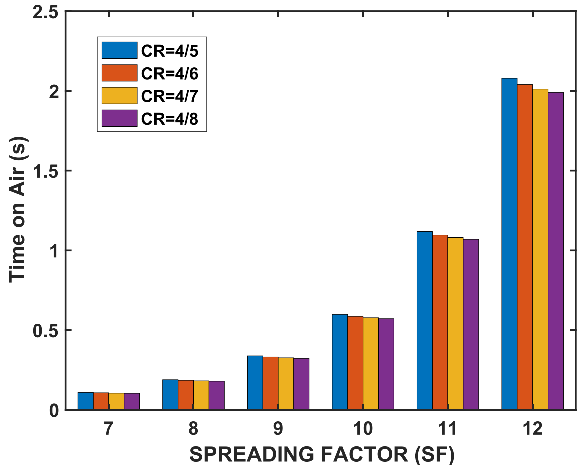

Fig. 2. Time on Air for various values of SF and CR for and CR for 44 bytes of a packet 44 bytes of a pack.

an Arduino Uno microcontroller to control the LoRa transmission parameters to transmit and receive the packets. It also shows the gateway module fortified with an SX1278 LoRa module and ESP32 microcontroller. The standard 3.6 dBi antenna is used for both the end device and the gateway and is configured to radiate with the transmission power of 14dBm throughout all the measurements. The specifications of the SX1278 LoRa module considered for the field tests are mentioned in Table 2.

In the experiment, a total of 1000 LoRa packets have been sent over a duration of 1 week to comply with LoRaWAN duty cycle restrictions and ensure efficient network performance. The system is configured to measure and transmit data every 10 min, adhering to duty cycle limitations to avoid surpassing regulatory requirements. The setup involves a prototype LoRa device with an SX1278 LoRa module operating at the frequency of 433 MHz. The end device, which transmits data, and the gateway, which receives data, are positioned 60 m apart. Both use a standard 3.6 dBi antenna, with the end device configured to transmit at 14 dBm. The SX1278 module is configured with a bandwidth of 125 kHz, a spreading factor (SF) ranging from 7 to 12, and coding rates (CR) of 4/5, 4/6, 4/7, and 4/8. By spacing out packet transmissions every 10 min throughout the week, the system adheres to LoRaWAN duty cycle constraints while ensuring effective data transmission over the fixed distance of 60 m.

4.2. Measurement setup

The indoor measurements are performed at three different locations in the engineering block of the AUGN campus, covering both LoS and NLoS scenarios within a fixed coverage area of 60m for all scenarios as shown in Fig. 4. Different constraints are considered to define the NLoS environment such as labs, classes with obstructions from concrete walls, wooden furniture, glass windows, and iron and steel railings (see).

During all measurements, the location of the gateway is fixed whereas the end device is positioned at various indoor locations (A, B & C) of the AUGN campus targeting to cover both LoS and NLoS environments. Fig. 5 shows the different locations of GW and the end device. For locations A & B, both the end device and the gateway were deployed on the third floor of the engineering block at a height of approximately 10m from the ground. Location A covers the LoS scenario with both the gateway and the prototype device placed in the corridors of the third floor without any obstruction between them. Location B is a highly obstructed location with the prototype device placed in a classroom with no line of sight with the gateway deployed in the lab. For location C, with the gateway deployed in the lab on the third floor of the

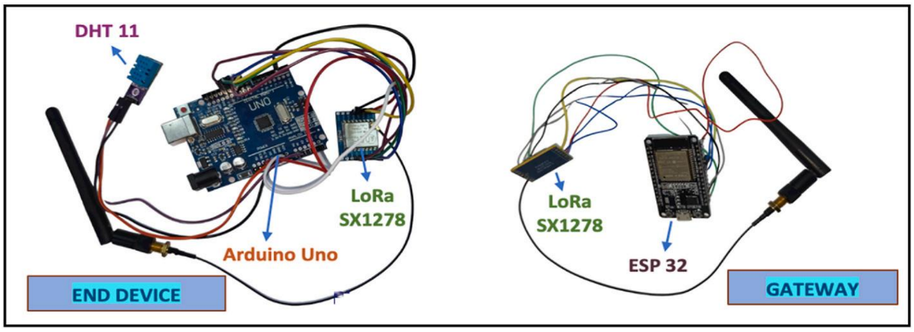

Fig. 3. Experimental setup used.

Table 2
Specification considered for SX1278 LoRa module.

Specification	Value
Bandwidth	125 kHz
Spreading Factor(SF)	7–12
Coding Rate (CR)	4/5, 4/6, 4/7 and 4/8
Transmission Power (dBm)	14 dBm
Carrier Frequency	433 MHz
Antenna	3.6 dBi

Fig. 4. Map of AUGN campus showing measurement locations of the end device and gateway.

engineering block, the end device is located on the first floor at a height of approximately 3m from the ground. At each location, the measurements are performed with both the end device and the gateway configured with the same LoRa parameter settings. The data symbols are transmitted with LoRa offering 3 optional bandwidths of 125 kHz, 250 kHz and 500 kHz. In our case, keeping the BW constant at 125 kHz, both the end device and the gateway cycle through in total of 24 combinations of transmission configuration with six SF values (7-12) and four CR values (4/5, 4/6, 4/7 and 4/8). The performance of the setup LoRaWAN network has been studied in terms of RSSI, SNR, and PRR. RSSI and SNR indicate the link quality of the network. PRR is determined as the ratio of transmitted packets to the received packets at the gateway which indicates the reliability of the communication link. Further using the PRR values the throughput of the setup network has been evaluated.

In the subsequent section, the methodology employed to record the measurements at the gateway has been discussed.

5. Measurement methodology

Through all sets of experiments at various locations on the campus, the influence of different LoRa configurations on the link quality and reliability of the network has been analysed. The results are confined within a distance of 60 m between the prototype LoRa end device and the gateway for both LoS and NLoS experiments.

The end device is configured to send 1000 packets with sequence numbers to identify the packet loss. The monitoring data from the prototype device was transmitted to the gateway device. Upon reception of each packet, the gateway provides the RSSI, SNR and payload message of 44 bytes indicating the temperature and humidity readings. The received packets are recorded on the receiving side for further processing and analysis. The implementation of the setup LoRaWAN network has been studied by referring to the LoRaWAN duty cycle restrictions that limit the allowable duration for the LoRa device to transmit.

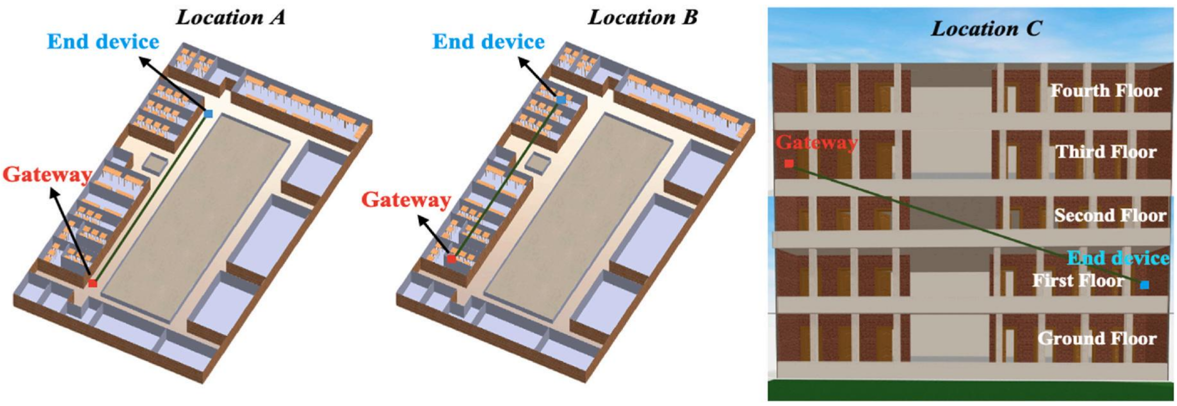

Fig. 5. Map of the indoor environment at AUGN campus showing the measurement locations of end device and gateway.

5.1. Reliability analysis

The registered data at the gateway for the LoRa packets transmitted from the prototype device is further utilized to analyse the reliability of the setup network pertaining to PRR and throughput. PRR is calculated as the ratio of the accurately received number of LoRa packets at the gateway to the number of packets transmitted by the end device. The value of PRR ranges from 0 to 1 with 0 denoting no reception of the LoRa packet and 1 indicating 100 % delivery accuracy. Further utilizing the registered values of PRR, throughput can be calculated. The achievable network throughput states the measure of information accurately received by the network and as stated in Ref. [42] is calculated as

$$\mathrm{Th} = \frac{\mathrm{PL} \times \lambda \times \mathrm{PRR}}{\mathrm{K}} \tag{5}$$

where, PL is the payload in bytes, λ is the packets generation rate per day and K is a constant specifying the number of seconds in a day.

6. Experimental results

For simulation work, all the tests are carried out on the same hardware and software platform.

6.1. Findings from indoor LoS environment (location A)

Figs. 6 and 7 illustrate the RSSI and the SNR respectively of the received signal at the gateway from the LoRa end device deployed at location A depicting the link quality of the LoRaWAN setup. The maximum RSSI and SNR values are achieved with LoRa configuration settings of SF = 9 and CR = 5 delivering the signal strength of −89.12 dBm and SNR value of 9.91 dB. However, the alternate setting with SF = 8 and CR = 6 can also be considered as it has a comparatively lower packet transmission time and higher data rate. However, this would depend upon the kind of IoT application's forbearance to noise and packet loss. If the application can abide by slight noise interference and one or few packet losses and simultaneously requires a higher data rate, then a little tough parameter setting could be exercised.

The reliability of the network can be investigated from Figs. 8 and 9 presenting PRR, and throughput respectively attained for the transmissions occurring from the LoRa device deployed at location A for diverging SF and CR values. From the figures, it is apparent that the parameter setting of SF = 11 gives 100 % packet delivery accuracy regardless of the CR values and thus providing maximum achievable throughput of 0.44 kbps for the setup. From the graphs is also quite

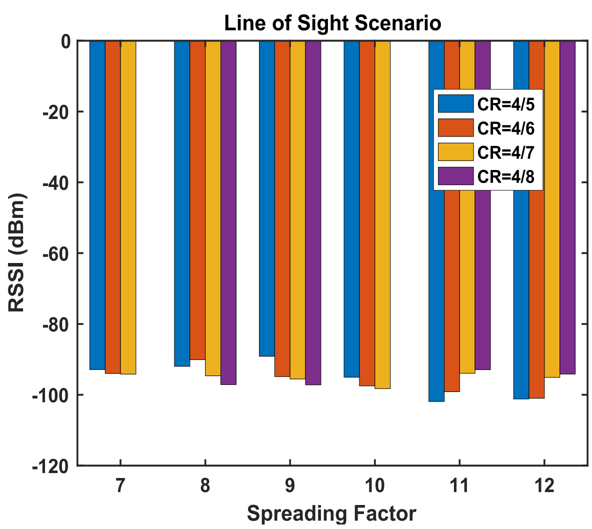

Fig. 6. RSSI recorded for various values of SF and CR.

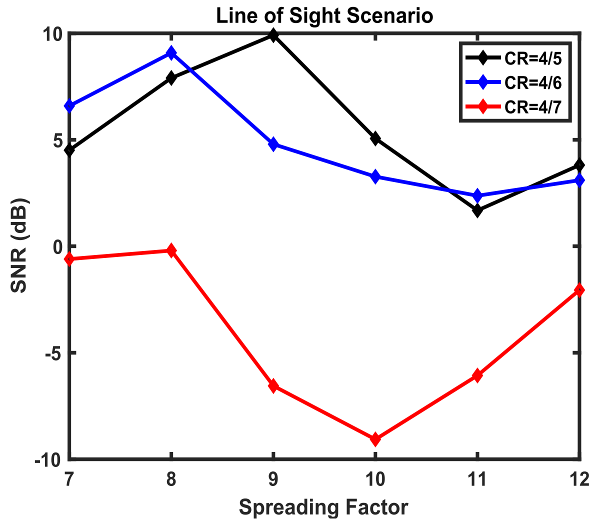

Fig. 7. SNR recorded for various values of SF and CR.

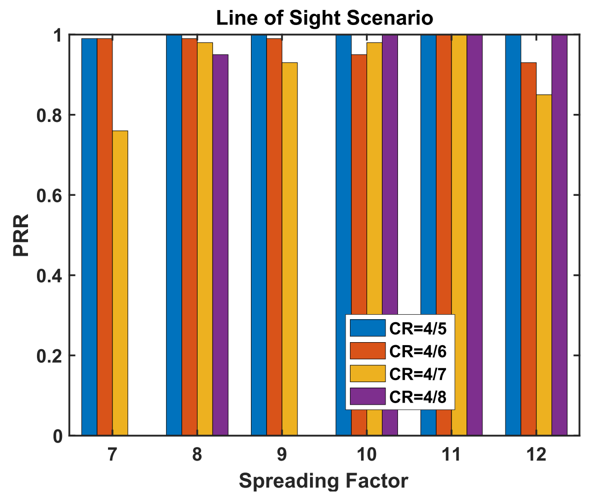

Fig. 8. PRR achieved for various values of SF and CR.

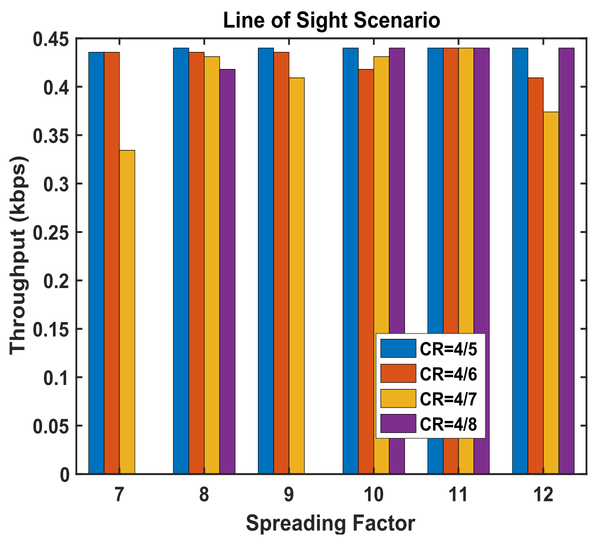

Fig. 9. Throughput achieved for various values of SF and CR.

evident that there is no obligation for higher redundancy to establish strong connectivity between the device and the gateway as maximum throughput and a PRR value of 1 could be attained with a lower value of CR = 4/5. No communication was possible with a higher CR value of 4/8 for SF = 7 and SF = 9 specifying the incompatibility of these permutations of SF and CR. As apparent from the graphs, the coding rate of 4/7 contributes to unreliable communication with few packet losses resulting in a PRR value of 0.76 with SF = 7 and 0.85 with SF = 12 thus providing the lowest throughput of the setup at this location.

6.2. Findings from the indoor highly obstructive environment (location B)

Location B is an indoor highly obstructive location with the gateway deployed in a lab and the prototype device placed in a classroom on the third floor of the engineering block with both the rooms located at the end of the block ensuring 60m of the straight-line distance between the transmitting and receiving ends. It is comparatively a vigorous environment with obstructions from the concrete walls and other materials like glass, iron and steel resulting in losses from signal penetrations through such obstructions. In addition to this human presence and movement were also there affecting the signal penetration through such obstructions. The verdicts from this location show that the maximum strength of the signal received at the gateway is −104.122 dBm as depicted in Fig. 10 for the configuration settings of SF = 7 and CR = 4/7.

Similar settings also depict the maximum SNR of the signal received at the gateway with a value of −10.19 dB as can be observed from Fig. 11. A comparable level of received signal strength is achieved at SF = 8 for the same level of redundancy (CR = 4/7) but as with an increase in SF the packet transmission time increases which add to signal degradation from the obstructions and noise. Subsequently, this results in the drop in SNR value of the signal at this configuration setting to −12.02 dB and packets delivery accuracy to 45 %. Thus, it entirely depends upon the type of IoT application to which configuration it must employ if it can accept noise interference and lower packet accuracy at the cost of a comparatively higher data rate.

Figs. 12 and 13 depict the PRR and throughput achieved from the transmission from location B at the gateway for different SF and CR settings. From the graphs, it can be observed that with SF = 11 and SF = 12, almost 100 % delivery of the packets is achieved resulting in maximum throughput of 0.44 kbps from the location regardless of the redundancy value. SF = 7 provides the maximum packet losses with 7 % and 10 % delivery accuracy with CR = 4/6 and CR = 4/7 and not even a single packet received with CR = 4/5 and CR = 4/8. This results in poor throughput with SF = 7 which implies weak communication with this configuration. With an increase in SF from 7 to 8 the PPR and

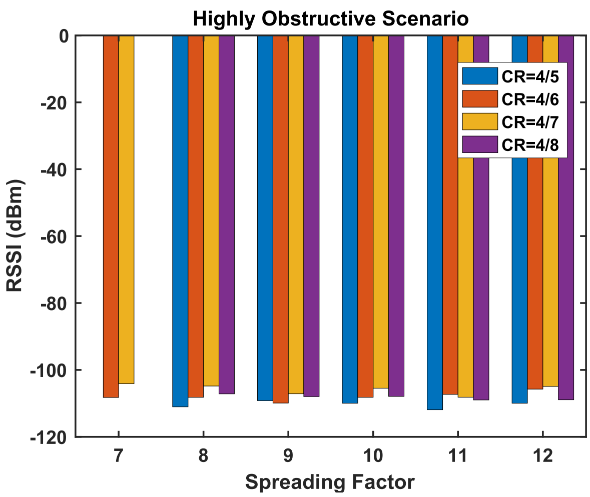

Fig. 10. RSSI recorded for various values of SF and CR.

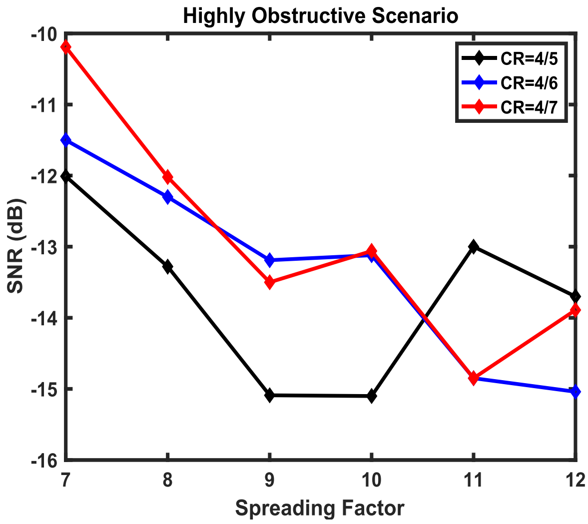

Fig. 11. SNR recorded for various values of SF and CR.

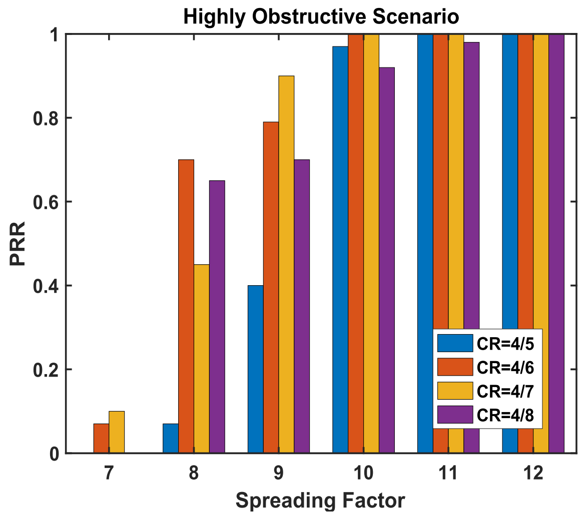

Fig. 12. PRR achieved for various values of SF and CR.

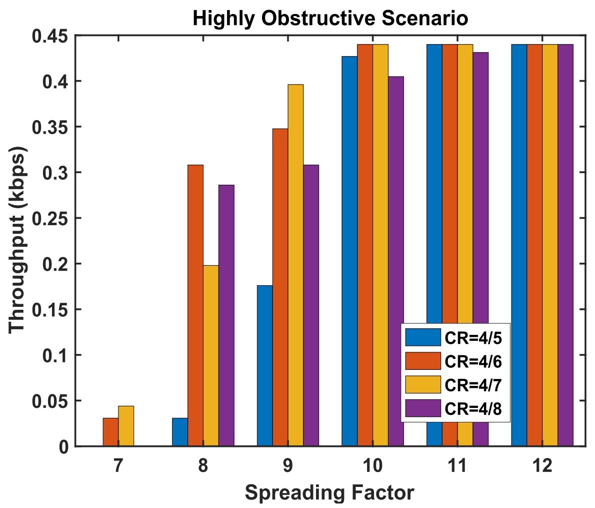

Fig. 13. Throughput achieved for various values of SF and CR.

throughput performance improves resulting in enhanced connectivity. As SF increases further, a remarkable improvement in PRR and throughput performance of the setup could be seen with CR = 4/6 and 4/7 thereby enhancing the reliability of the communication.

6.3. Findings from the indoor obstructive environment (location C)

Location C is an indoor obstructive location with the gateway deployed in a lab on the third floor and the prototype end device deployed diagonally at a straight-line distance of approximately 60m from the gateway on the first floor of the same building. The signal from this location has to penetrate through the floors and other similar obstructions confronted in the previous location to reach the gateway placed two floors diagonally above the end device. Due to such obstructions in the path of signal transmissions, multipath fading cannot be disregarded. Figs. 14 and 15 present the RSSI and the SNR respectively of the received signal at the gateway for location C describing the link quality of the setup. From the graphs, it is quite apparent that although SF = 8 and CR = 4/5 give the maximum RSSI value of −101.25 dBm but offer high packet loss with hardly two packets received for the said configuration. An almost similar level of signal strength is achieved with the same SF but with the redundancy of 4/7 providing −101.99 dBm of RSSI value and 99 % delivery accuracy and SNR of −8.19 dB due to noise interference.

The maximum recorded SNR value for this location is −3.94 dB with transmission configuration of SF = 7 and CR = 4/8 with low TOA, high data rate and 100 % delivery accuracy. The reliability of the network could be witnessed from Figs. 16 and 17 illustrating the PRR and throughput of the setup. From the graphs, it could be observed that SF = 10 and SF = 11 offer the maximum PRR value of 1 and maximum achievable throughput of 0.44 kbps irrespective of the CR values. Not even a single packet is received with CR = 4/6 and SF = 7 to SF = 9 whereas for SF = 7 and CR = 4/5 single packet is received specifying no communication possible with these sets of configurations.

Although disregarding CR = 4/6, the PRR and throughput of the setup increase with an increase in SF but it degrades for SF = 12 with close to 60 % delivery accuracy for all redundancy values except for CR = 4/5 offering 0 PRR. This indicates the unsuitability of SF = 12 for reliable communication to occur. The fluctuation of the recorded RSSI values of the LoRa packets received at the gateway located at three different locations is presented by the histogram and cumulative distribution function (CDF) of the RSSI values in Figs. 18 and 19 respectively. Table 3 shows the maximum and minimum values of performance metrics recorded at each location.

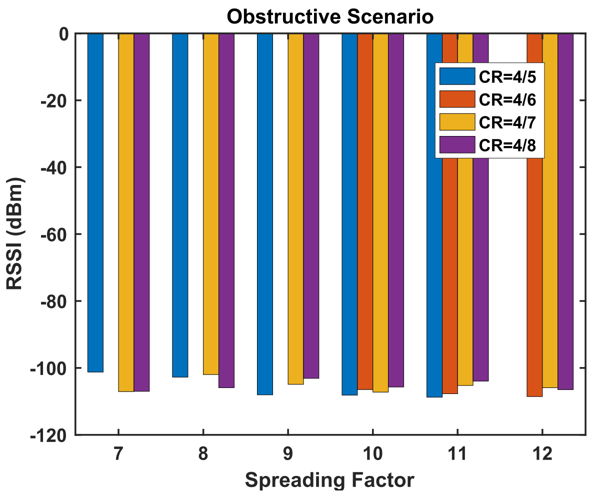

Fig. 14. RSSI recorded for various values of SF and CR.

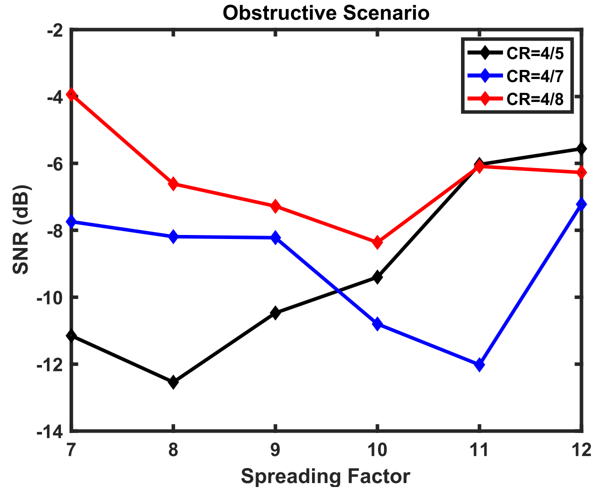

Fig. 15. SNR recorded for various values of SF and CR.

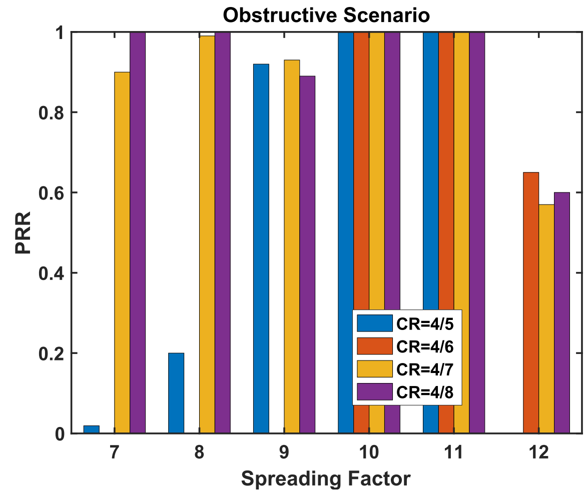

Fig. 16. PRR achieved for various values of SF and CR.

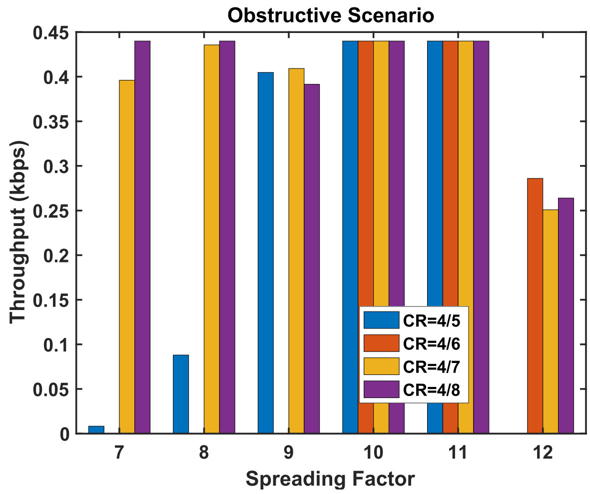

Fig. 17. Throughput achieved for various values of SF and CR.

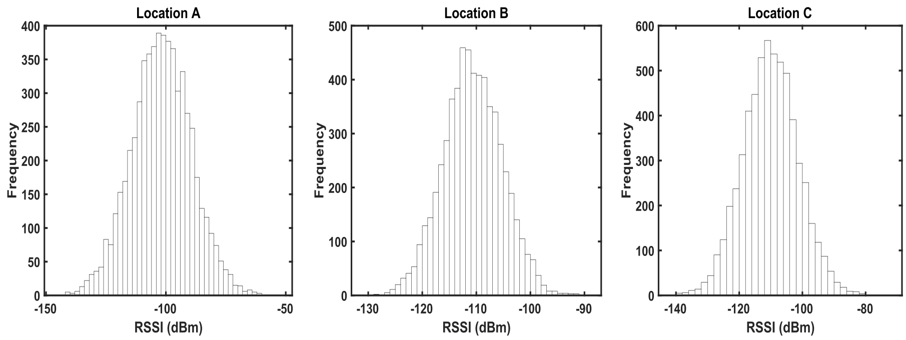

Fig. 18. Histogram of RSSI values recorded at three different indoor locations.

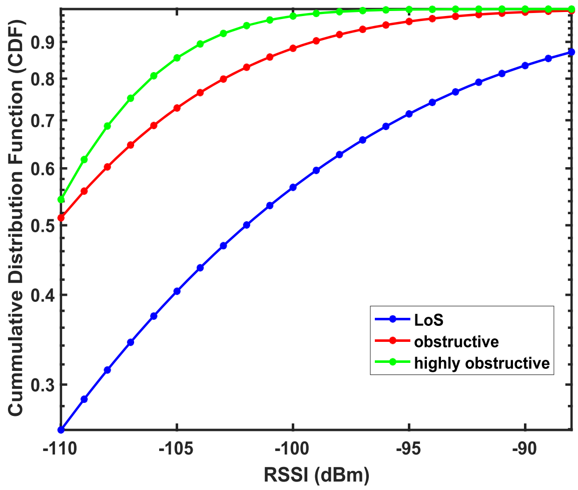

Fig. 19. CDF of RSSI values recorded for different scenarios.

7. Discussion

7.1. Indoor LoS environment (location A)

In a Line-of-Sight (LoS) environment, where there are minimal obstructions and interference, the configuration of SF = 9 and CR = 4/5 is optimal. It delivers an RSSI of −89.12 dBm and an SNR of 9.91 dB, providing a strong signal and an notable signal-to-noise ratio. The SF of 9 strikes a balance between range and data rate, ensuring robust signal transmission over moderate distances. The CR of 4/5 upholds a high data rate with minimal redundancy, making it well-suited for environments where signal clarity is crucial. Ultimately, this configuration guarantees efficient and dependable communication in non-obstructive conditions.

However, SF = 11 ensures 100 % packet delivery accuracy due to its longer time on air (TOA) with maximum throughput of 0.44 kbps. A higher SF increases the duration of each bit transmitted, which enhances signal sensitivity and allows for better detection amidst noise and interference. This makes SF = 11 suitable for scenarios where reliability is prioritized over data rate.

7.2. Indoor highly obstructive environment (location B)

In highly obstructive indoor environments with significant physical barriers and interference, SF = 7 and CR = 4/7 could be the finest settings for managing signal strength and integrity. SF = 7 results in a higher data rate and shorter transmission time, thereby reducing the probability of interference and thus improving signal clarity. Meanwhile, CR = 4/7 provides a balanced level of error correction, effectively ensuring both robustness and efficiency.

To achieve 100 % packet delivery accuracy in such challenging environments, SF = 11 and SF = 12 could be effective due to the extended spreading factor, maximizing the signal robustness at the expense of data rate.

7.3. Indoor obstructive environment

In environments with less obstructions, with fewer barriers to signal transmission, SF = 8 and CR = 4/7 bring a balanced performance with an RSSI of −101.99 dBm and an SNR of −8.19 dB. This configuration ensures good signal strength and error correction while upholding a reasonable data rate.

To maximize PRR and throughput, SF = 10 and SF = 11 has proved to be the most effective. SF = 10 offers a good balance between range and data rate.

8. Conclusion

The current work focusses on exploring the implementation of the LoRaWAN network through an experimental setup deployed on the campus of Amity University, Greater Noida, India. Extensive measurements are taken by deploying the prototype device at different indoor locations on the campus covering LoS and NLoS propagation scenarios affected by multipath propagation and obstructions. The experiment was conducted with the end device transmitting packets considering duty cycle restrictions. The prototype device and the gateway integrate the SX1278 LoRa radio module operating at a frequency of 433 MHz. The performance of the deployed setup is analysed in terms of link quality and reliability. The study highlights that the performance of the network is sensitive to the choice of parameter configuration setting

Table 3
Performance metrics recorded from each location.

Location	Scenario	RSSI (dBm)		SNR (dB)		PRR		Throughput (kbps)	
		Max.	Min.	Max.	Min.	Max.	Min.	Max.	Min.
A	LoS	−89.12	−101.97	9.91	−9.07	1	0	0.44	0
B	highly obstructive	−104.12	−111.91	−10.19	−15.10	1	0	0.44	0
C	obstructive	−101.25	−108.74	−3.94	−12.54	1	0	0.44	0

depending upon the deployment scenario. There are situations where the choice of hardline parameter settings provides better connectivity at the cost of an increase in packet transmission duration of the packet resulting in an increased risk of noise interference and collisions. Identifying the optimal transmission configuration and adapting them to provide enhanced network performance in any of the deployment scenarios is the challenge.

For LoS environment, the maximum RSSI and SNR values are achieved with configuration settings of SF = 9, CR = 5 delivering a signal strength of −89.12 dBm and SNR value of 9.91 dB. On the contrary, SF = 11 offers good reliability as it delivers 100 % packet delivery accuracy regardless of the CR values thus providing a maximum achievable throughput of 0.44 kbps. For a highly obstructive indoor area, the maximum signal strength is received at configuration settings of SF = 7 and CR = 4/7 with RSSI = 104.122 dBm and SNR value of −10.19 dB. In this scenario, SF = 11 and SF = 12 provide 100 % packet delivery accuracy and maximum achievable throughput. For less obstructive scenario, SF = 8 and CR = 4/7 offer −101.99 dBm of RSSI value and SNR of −8.19 dB. For this case, it has been observed that SF = 10 and SF = 11 contributes to the maximum PRR and achievable throughput.

In the current work, LoRa has revealed robust performance in upholding reliable communication even over shorter indoor distances. The results specify that LoRa efficiently handles signal propagation through obstructions and varying indoor conditions, accomplishing reliable connectivity in scenarios where other technologies might face challenges. This performance recommends that LoRa can be beneficial in complex indoor environments, offering reliable and steady communication even over shorter distances, where traditional technologies might struggle with signal strength and reliability.

Future work will investigate the network performance in outdoor deployments as well as indoor-outdoor deployments for varying coverasge areas with more LoRa nodes. The range and performance trade-off to meet the operational cost benefits and commercial requirements will also be considered.

Funding

Not Applicable.

Availability of data and material

Not Applicable.

Code availability

Yes.

CRediT authorship contribution statement

Gagandeep Kaur: Writing – original draft, Visualization, Methodology, Formal analysis, Data curation, Conceptualization. **Vipin Balyan:** Writing – review & editing, Visualization, Validation, Supervision, Investigation, Formal analysis. **Sindhu Hak Gupta:** Writing – review & editing, Visualization, Validation, Supervision, Investigation, Conceptualization.

Declaration of competing interest

The authors declare that they have no known competing financial interests or personal relationships that could have appeared to influence the work reported in this paper.

Data availability

The data that has been used is confidential.

References

[1] Global Internet of Things (IoT) Market Size To Hit USD, (n.d.). https://www.globenewswire.com/news-release/2022/01/13/2366783/0/en/Global-Internet-of-Things-IoT-Market-Size-To-Hit-USD-1-842-Billion-by-2028-at-a-24-5-CAGR-Growth-with-COVID-19-Analysis-Facts-Factors.html.(accessed October 3, 2022).

[2] D.A. Verde Romero, E. Villalvazo Laureano, R.O. Jiménez Betancourt, E. Navarro Álvarez, An open source IoT edge-computing system for monitoring energy consumption in buildings, Results in Engineering 21 (2024) 101875, https://doi.org/10.1016/J.RINENG.2024.101875.

[3] A. Mathur, T. Newe, W. Elgenaidi, M. Rao, G. Dooly, D. Toal, A secure end-to-end IoT solution, Sens Actuators A Phys 263 (2017) 291–299, https://doi.org/10.1016/j.sna.2017.06.019.

[4] S.S. Salwe, K.K. Naik, Heterogeneous wireless network for IoT applications, IETE Tech. Rev. 36 (2019) 61–68, https://doi.org/10.1080/02564602.2017.1400412.

[5] U. Raza, P. Kulkarni, M. Sooriyabandara, Low power wide area networks: an overview, IEEE Communications Surveys and Tutorials 19 (2017) 855–873, https://doi.org/10.1109/COMST.2017.2652320.

[6] G. Kaur, S.H. Gupta, H. Kaur, An approach to optimize LoRa network performance for efficient IoT applications, Wireless Pers. Commun. (2022), https://doi.org/10.1007/s11277-022-09950-1.

[7] M.A. Ertürk, M.A. Aydın, M.T. Büyükakkaşlar, H. Evirgen, A survey on LoRaWAN architecture, protocol and technologies, Future Internet 11 (2019) 216, https://doi.org/10.3390/FI11100216.

[8] A. Ikpehai, B. Adebisi, K.M. Rabie, K. Anoh, R.E. Ande, M. Hammoudeh, H. Gacanin, U.M. Mbanaso, Low-power wide area network technologies for internet-of-things: a comparative review, IEEE Internet Things J. 6 (2019) 2225–2240, https://doi.org/10.1109/JIOT.2018.2883728.

[9] K. Mekki, E. Bajic, F. Chaxel, F. Meyer, A comparative study of LPWAN technologies for large-scale IoT deployment, ICT Express 5 (2019) 1–7, https://doi.org/10.1016/J.ICTE.2017.12.005.

[10] H. Cho, Personal environmental monitoring system and network platform. Proceedings of the International Conference on Sensing Technology, ICST 2016-March, 2016, pp. 751–756, https://doi.org/10.1109/ICSENST.2015.7438496.

[11] J.P. Smith, X. Li, AirSniffer: a smartphone-based sensor system for body area climate and air quality monitoring. International Symposium on Medical Information and Communication Technology, ISMICT 2016-June, 2016, https://doi.org/10.1109/ISMICT.2016.7498910.

[12] T.V. Tran, N.T. Dang, W.Y. Chung, Battery-free smart-sensor system for real-time indoor air quality monitoring, Sens Actuators B Chem 248 (2017) 930–939, https://doi.org/10.1016/J.SNB.2017.01.198.

[13] A. Martín-Garín, J.A. Millán-García, A. Baïri, J. Millán-Medel, J.M. Sala-Lizarraga, Environmental monitoring system based on an Open Source Platform and the Internet of Things for a building energy retrofit, Autom Constr 87 (2018) 201–214, https://doi.org/10.1016/J.AUTCON.2017.12.017.

[14] A. Moreno-Rangel, T. Sharpe, F. Musau, G. McGill, Field evaluation of a low-cost indoor air quality monitor to quantify exposure to pollutants in residential environments, Journal of Sensors and Sensor Systems 7 (2018) 373–388, https://doi.org/10.5194/JSSS-7-373-2018.

[15] X. Yang, L. Yang, J. Zhang, A WiFi-enabled indoor air quality monitoring and control system: the design and control experiments. IEEE International Conference on Control and Automation, ICCA, 2017, pp. 927–932, https://doi.org/10.1109/ICCA.2017.8003185.

[16] A. Carre, T. Williamson, Design and validation of a low cost indoor environment quality data logger, Energy Build. 158 (2018) 1751–1761, https://doi.org/10.1016/J.ENBUILD.2017.11.051.

[17] M. Karami, G.V. McMorrow, L. Wang, Continuous monitoring of indoor environmental quality using an Arduino-based data acquisition system, J. Build. Eng. 19 (2018) 412–419, https://doi.org/10.1016/J.JOBE.2018.05.014.

[18] C.T. Yang, S.T. Chen, W. Den, Y.T. Wang, E. Kristiani, Implementation of an intelligent indoor environmental monitoring and management system in cloud, Future Generat. Comput. Syst. 96 (2019) 731–749, https://doi.org/10.1016/J.FUTURE.2018.02.041.

[19] Z. Liu, Y. Li, L. Zhao, R. Liang, P. Wang, Comparative evaluation of the performance of ZigBee and LoRa wireless networks in building environment, Electronics 11 (2022) 3560, https://doi.org/10.3390/ELECTRONICS11213560, 3560 11 (2022).

[20] L. Kane, V. Liu, M. McKague, G. Walker, An experimental field comparison of wi-fi HaLow and LoRa for the smart grid, Sensors 23 (2023) 7409, https://doi.org/10.3390/S23177409. Page 7409 23 (2023).

[21] L. Bai, F. Ciravegna, R. Bond, M. Mulvenna, A low cost indoor positioning system using Bluetooth low energy, IEEE Access 8 (2020) 136858–136871, https://doi.org/10.1109/ACCESS.2020.3012342.

[22] M.O. Ojo, D. Adami, S. Giordano, Experimental evaluation of a LoRa wildlife monitoring network in a forest vegetation area, Future Internet 13 (2021) 115, https://doi.org/10.3390/FI13050115. Page 115 13 (2021).

[23] O. Elijah, S.K.A. Rahim, V. Sittakul, A.M. Al-Samman, M. Cheffena, J. Bin Din, A. R. Tharek, Effect of weather condition on LoRa IoT communication technology in a tropical region: Malaysia, IEEE Access (2021), https://doi.org/10.1109/access.2021.3080317, 1–1.

[24] A.P.A. Torres, C.B. Da Silva, H.T. Filho, An experimental study on the use of LoRa technology in vehicle communication, IEEE Access 9 (2021) 26633–26640, https://doi.org/10.1109/ACCESS.2021.3057602.

[25] K. Lin, T. Hao, Experimental link quality analysis for LoRa-based wireless underground sensor networks, IEEE Internet Things J. 8 (2021) 6565–6577, https://doi.org/10.1109/JIOT.2020.3044647.

[26] S.Z.A. Mehdi, A. Mohd, A. Zulkifli, S. Lorawan Cubesat, LoRaWAN CubeSat with an adaptive data rate: an experimental analysis of path loss link margin, Aerospace 10 (2023) 53, https://doi.org/10.3390/AEROSPACE10010053. Page 53 10 (2023).
[27] Q. Guo, F. Yang, J. Wei, Experimental evaluation of the packet reception performance of LoRa, Sensors 21 (2021) 1071, https://doi.org/10.3390/S21041071. Page 1071 21 (2021).
[28] P. Kulkarni, Q.O.A. Hakim, A. Lakas, Experimental evaluation of a campus-deployed IoT network using LoRa, IEEE Sens J 20 (2020) 2803–2811, https://doi.org/10.1109/JSEN.2019.2953572.
[29] M.J. Faber, K.M. Van Der Zwaag, W.G.V. Dos Santos, H.R.D.O. Rocha, M.E. V. Segatto, J.A.L. Silva, A theoretical and experimental evaluation on the performance of LoRa technology, IEEE Sens J 20 (2020) 9480–9489, https://doi.org/10.1109/JSEN.2020.2987776.
[30] R. Liang, L. Zhao, P. Wang, Performance evaluations of LoRa wireless communication in building environments, Sensors 20 (2020) 3828, https://doi.org/10.3390/S20143828. Page 3828 20 (2020).
[31] A. Vazquez-Rodas, F. Astudillo-Salinas, C. Sanchez, B. Arpi, L.I. Minchala, Experimental evaluation of RSSI-based positioning system with low-cost LoRa devices, Ad Hoc Netw. 105 (2020) 102168, https://doi.org/10.1016/J.ADHOC.2020.102168.
[32] B. Abdallah, S. Khriji, R. Chéour, C. Lahoud, K. Moessner, O. Kanoun, Improving the reliability of long-range communication against interference for non-line-of-sight conditions in industrial internet of things applications, Appl. Sci. 14 (2024) 868, https://doi.org/10.3390/APP14020868. Page 868 14 (2024).
[33] N.C. Lopes, R. Alexandre, A. Ramos, L. Miguel, R. Pires, LoRa network-based IoT node for indoor environment monitoring, Brazilian Journal of Development 10 (2024) e69915, https://doi.org/10.34117/BJDV10N5-058.
[34] L. Aarif, M. Tabaa, H. Hachimi, Performance evaluation of LoRa communications in harsh industrial environments, J. Sens. Actuator Netw. 12 (2023) 80, https://doi.org/10.3390/JSAN12060080. Page 80 12 (2023).
[35] R. Robles-Enciso, I.P. Morales-Aragón, A. Serna-Sabater, M.T. Martínez-Inglés, A. Mateo-Aroca, J.M. Molina-Garcia-Pardo, L. Juan-Llácer, LoRa, zigbee and 5G propagation and transmission performance in an indoor environment at 868 MHz, Sensors 23 (2023) 3283, https://doi.org/10.3390/S23063283. Page 3283 23 (2023).
[36] C. Zhong, X. Nie, Feasibility of LoRa for smart home: real time and coverage considerations, IEEE Internet Things J. (2024), https://doi.org/10.1109/JIOT.2024.3391761.
[37] R.O. Andrade, S.G. Yoo, A comprehensive study of the use of LoRa in the development of smart cities, Appl. Sci. 9 (2019) 4753, https://doi.org/10.3390/app9224753.
[38] R.M. Sandoval, A.J. Garcia-Sanchez, J. Garcia-Haro, Optimizing and updating LoRa communication parameters: a Machine Learning approach, IEEE Transactions on Network and Service Management 16 (2019) 884–895, https://doi.org/10.1109/TNSM.2019.2927759.
[39] H. Taleb, A. Nasser, G. Andrieux, N. Charara, E.M. Cruz, Energy consumption improvement of a healthcare monitoring system: application to LoRaWAN, IEEE Sens J 22 (2022) 7288–7299, https://doi.org/10.1109/JSEN.2022.3150716.
[40] T. Bouguera, J.F. Diouris, J.J. Chaillout, R. Jaouadi, G. Andrieux, Energy consumption model for sensor nodes based on LoRa and LoRaWAN, Sensors 18 (2018) 2104, https://doi.org/10.3390/S18072104. Page 2104 18 (2018).
[41] S. Bagwari, A. Roy, A. Gehlot, R. Singh, N. Priyadarshi, B. Khan, LoRa based metrics evaluation for real-time landslide monitoring on IoT platform, IEEE Access 10 (2022) 46392–46407, https://doi.org/10.1109/ACCESS.2022.3169797.
[42] L. Feltrin, C. Buratti, E. Vinciarelli, R. De Bonis, R. Verdone, LoRaWAN: evaluation of link- and system-level performance, IEEE Internet Things J. 5 (2018) 2249–2258, https://doi.org/10.1109/JIOT.2018.2828867.